

3 **Role of the surface chemistry of the adsorbent on the**  
4 **initialization step of the water sorption process**

5  
6 Leticia F. Velasco<sup>1\*</sup>, Didier Snoeck<sup>2,3</sup>, Arn Mignon<sup>2,3</sup>, Lara Misseeuw<sup>4</sup>, Conchi O. Ania<sup>5</sup>, Sandra Van  
7 Vlierberghe<sup>3,4</sup>, Peter Dubruel<sup>3</sup>, Nele de Belie<sup>2</sup>, Peter Lodewyckx<sup>1</sup>

8  
9 <sup>1</sup>Department of Chemistry, Royal Military Academy, Renaissancelaan 30, 1000 Brussels, Belgium.

10 <sup>2</sup>Magnel Laboratory for Concrete Research, Ghent University, Technologiepark Zwijnaarde 904,  
11 B-9052, Ghent, Belgium.

12 <sup>3</sup>Polymer Chemistry and Biomaterials Group, Ghent University, Krijgslaan 281 (S4) B-9000, Ghent,  
13 Belgium.

14 <sup>4</sup>Brussels Photonics Team, Vrije Universiteit Brussel, Pleinlaan 2, 1050 Elsene, Belgium.

15 <sup>5</sup>ADPOR Group, Instituto Nacional del Carbón (INCAR), Consejo Superior de Investigaciones  
16 Científicas (CSIC), Apdo. 73, 33080 Oviedo, Spain

17  
18  
19 \*Corresponding author. Tel.: +32(0)24414168. E-mail address: leticia.fernandez@mil.be (LF  
20 Velasco).

22

23

24

25 **Abstract**

26

27 In this work, an equation for the prediction of the low pressure region of the water adsorption  
28 isotherms of activated carbons, based on their amount of surface groups, has been further developed  
29 in order to account for porous carbonaceous materials with an oxygen-rich surface chemistry. To  
30 attain this goal, highly hydrophilic carbon materials were selected and their surface chemistry was  
31 modified by several techniques (mainly thermal and plasma treatments) in order to obtain a series of  
32 samples with a surface oxygen content up to 45 wt. %. Then, their water sorption isotherms were  
33 measured and the amount of surface groups obtained by fitting them by the proposed equation was  
34 compared with the one resulting from direct X-ray photoelectron spectroscopy (XPS) measurements.  
35 Based on the obtained results, it seems that beyond a certain concentration of surface oxygen, there is  
36 a change in the sorption mechanism (from clustering to layering) and consequently, on the size of the  
37 water cluster formed before the micropore filling. These findings have allowed us to go a step further  
38 in the modelling of this part of the water sorption isotherms and to find a correlation between the  
39 surface oxygen content and the water cluster size.

40

41

42

43

44

45

46

47

48

49

50

## 51 **1. Introduction**

52 In recent years a number of experimental and simulation studies of adsorption of water in porous  
53 materials have appeared in the literature [1-6]. However, the mechanism of water adsorption is not  
54 yet fully understood and is still subject of discussion [1,4].

55 This work focuses on the low pressure range of the water sorption isotherms, prior to the start of  
56 micropore filling. The shape of the water isotherm is here affected by the specific interactions  
57 (hydrogen bonding) between the water molecules and the active sites on the carbon surface, followed  
58 by a water cluster growth (again by hydrogen bridging) on these initially bound water molecules.  
59 Thus, at very low loadings, water molecules adsorb around the functional groups at the edges of the  
60 graphene layers due to the strong electrostatic interactions, compared to the intermolecular  
61 interactions and the interactions between water and the graphene layer. As the loading is increased,  
62 water clusters are formed around the functional groups and grow in size because of the greater  
63 electrostatic interactions between water molecules compared to the dispersive water-graphene  
64 interactions [7].

65 Based on previous works [8-11], where the above-described initiation and growth of the water  
66 clusters has been modelled, a Langmuir-type equation (Eq. 1) was proposed to accurately fit the  
67 low-pressure range of the water adsorption isotherms [12]:

$$W = \frac{5[O + N][O + N](p/p_o)}{1 + [O + N](p/p_o)} \quad \text{Equation 1}$$

68 with  $W$  the amount of water adsorbed (g/g),  $p/p_0$  the partial water pressure and  $[O+N]$  the amount of  
69 surface (oxygenated and nitrogenated) complexes expressed as  $g/g_{\text{carbon}}$ . In this regard, X-ray  
70 Photoelectron Spectroscopy (XPS) is a suitable technique for measuring this last variable since it

71 allows to quantify the functionalities located on the surface of the material (and not in the matrix), and  
72 therefore available to participate in the water sorption process [13].

73 In this first approach [12], the values of [O+N] obtained by fitting the water vapour isotherms of a  
74 considerable number of samples by Eq. 1 were compared with those resulting from XPS  
75 measurements and it was shown that the model gives good to excellent results for activated carbons  
76 with [O+N] up to 16 %. However, when trying to apply it to materials with a richer surface chemistry,  
77 Eq. 1 does not seem to be valid in its present form.

78 In this work, and taking into account recent investigations where it was shown that oxygen groups  
79 play a dominant role on the water adsorption process [14,15], we have focused on the influence of  
80 these functionalities on the initialization mechanism. Specifically, it is necessary to determine if – in  
81 the case of materials with an oxygen-rich surface chemistry – the mechanism of micropore filling also  
82 proceeds through the formation of clusters of five water molecules [10,11] or, on the contrary, the  
83 equation should be modified as a function of oxygen content.

84 For this reason, different porous carbonaceous materials with an oxygen-rich surface chemistry and  
85 almost negligible nitrogen content were selected. Therefore, the [O+N] factor of Eq. 1 will be labelled  
86 as [O] hereinafter. Among the studied materials are activated carbons, resorcinol-formaldehyde  
87 carbonaceous resins (which present high surface oxygen contents difficult to achieve with activated  
88 carbons) and cements. The four main reasons behind the selection of the latter are: i) the  
89 carbonaceous nature of the materials with ii) high oxygen contents due to the high relative presence of  
90 hydrates and oxides within their composition. However, the final oxygen and carbon content can also  
91 vary from sample to sample depending on the preparation procedure, hydration time, the use of  
92 additives, the drying method...[16]. Moreover, iii) they can be considered as porous materials, with  
93 specific surface areas around 80-140 m<sup>2</sup>/g (but also dependent on the previously mentioned  
94 parameters) [17]. This porosity is mainly due to the formation of the calcium-silicate-hydrate phase  
95 during the hydration of the cement, which contains a network of fine pores called gel pores [18].

96 Finally, iv) including cements in our study will allow us to broaden the applicability of the model  
97 towards a wider variety of porous carbonaceous materials.

98 Moreover, the surface chemistry of some of the parent materials was modified by thermal and plasma  
99 treatments (described in the experimental section) in order to obtain a series of samples with an  
100 increasing surface oxygen content of 17 to 45 wt.%. Then, their water sorption isotherms were  
101 measured and the initial equation was modified according to the obtained results.

102 Summing up, the present study provides further insights on the role played by the surface oxygen  
103 groups on the initialization step of the water vapour sorption process in porous carbonaceous  
104 materials and, consequently, it has allowed us to go a step further in the modelling of the water  
105 sorption isotherms.

## 106 **2. Experimental**

107 Carbonaceous resins (samples CR70 and CR85) were prepared following the same experimental  
108 procedure [19,20] (sol-gel polymerization of resorcinol and formaldehyde in water, using sodium  
109 carbonate as catalyst) but with different gelation temperatures (70 and 85°C, respectively). This  
110 synthesis method leads to carbon materials with a surface rich in polar and reactive oxygen groups  
111 [21, 22]. Specifically, samples CR70 and CR85 are characterized (Table 1) by a very similar and high  
112 oxygen content (~ 31 wt. %), an almost negligible nitrogen content ( $\leq 0.05$  wt. %). They also present  
113 a highly developed porosity ( $S_{\text{BET}} = 489$  and  $591 \text{ m}^2/\text{g}$ , respectively). Then, sample CR70 was further  
114 submitted to thermal treatments under nitrogen atmosphere (50 mL/min) at 200, 450 and 700°C for 1  
115 hour in order to selectively remove its surface groups and thus obtaining three materials (CR70 H200,  
116 CR70 H450, CR70 H700) with intermediate oxygen contents.

	<b>XPS (wt. %)</b>		
	<b>C</b>	<b>N</b>	<b>O</b>
<b>CR70</b>	64.5	0.01	30.9
<b>CR85</b>	65.5	0.05	31.9

117 **Table 1.** Surface chemistry characterization of the carbonaceous resins (CR70 and CR85).

118 CR70, CR70 H450 and activated carbon 362 (which was the activated carbon with the highest surface  
119 oxygen content selected for the previous study [12] and with a  $S_{\text{BET}} = 1076 \text{ m}^2/\text{g}$ ) were also subjected  
120 to plasma treatments in argon and oxygen atmospheres (samples PAr and PO<sub>2</sub>, respectively) in a  
121 cylindrical dielectrical discharge plasma reactor (Model Femto, version 3, Diener Electronic,  
122 Germany). The gas pressure was kept at 0.8 mbar and the applied power was 100 W. This technique  
123 offers potential advantages for the surface modification of carbon materials while preserving their  
124 textural properties [23,24].

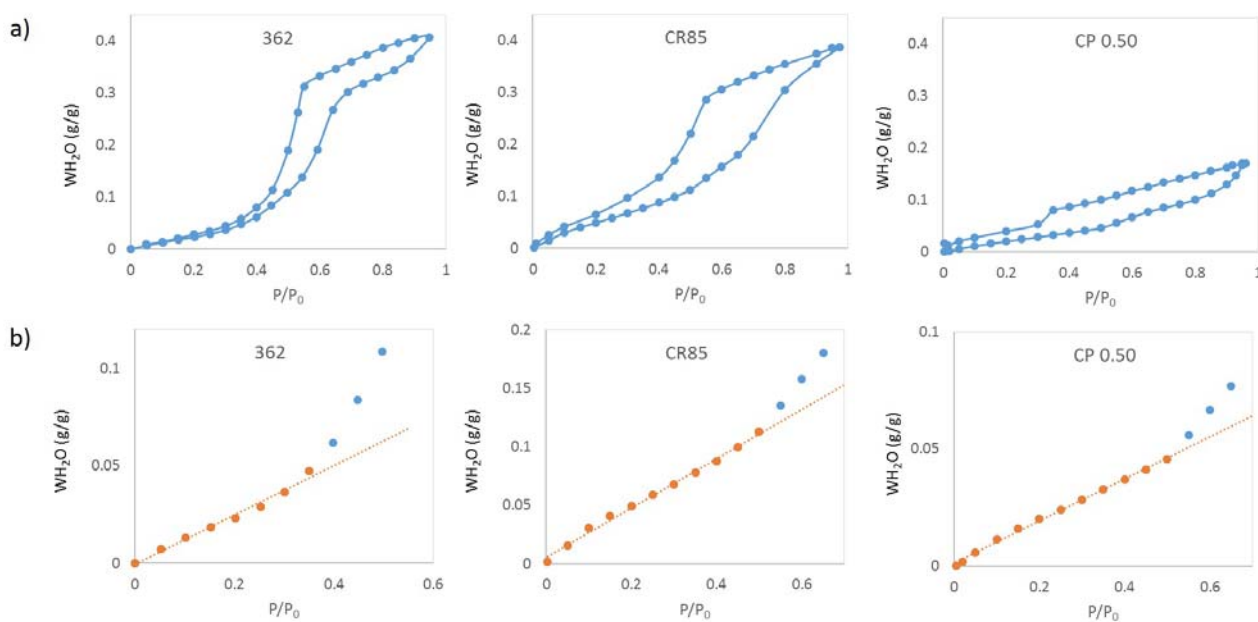
125 Finally, two cement pastes with different water-to-cement ratios were made and cast [17]. The  
126 cement used was CEM I 52.5 N and the standard used for the mixing procedure was EN 196-1. The  
127 chemical and phase composition of the cement can be found elsewhere [17,25]. After one day of  
128 storage in a relative humidity of  $95 \pm 5\%$  and a temperature of  $20 \pm 2^\circ\text{C}$ , the samples were stored in  
129 water at  $20 \pm 2^\circ\text{C}$  for a minimum period of 6 months to ensure a stable formation of the cementitious  
130 matrix. Prior to testing, the samples were ground and sieved (500 - 1000  $\mu\text{m}$ ). The nomenclature  
131 given to these samples is CP followed by a number which stands for their water-to-cement ratio.

132 Dynamic water vapour sorption (DVS) isotherms of all the studied materials were performed in a  
133 gravimetric water sorption analyzer (Aquadyne DVS, Quantachrome). Before the sorption  
134 experiments, the activated carbons and carbonaceous resins were outgassed under temperature  
135 ( $120^\circ\text{C}$ ) and vacuum ( $10^{-5}$  Torr) for 24 hours. In the case of cement pastes, and in order to preserve  
136 their microstructural properties, the samples were prepared for the analysis using a  
137 solvent-exchange-method in isopropanol followed by vacuum drying at  $20^\circ\text{C}$  as further detailed in  
138 [17]. The amount of surface-oxygenated groups of the materials was measured by XPS, under high  
139 vacuum conditions, using an ESCA S-probe VG monochromatic spectrometer with an Al  $K\alpha$  X-ray  
140 source (1486 eV), recorded with a spot size of 250  $\mu\text{m}$  by 1000  $\mu\text{m}$  and analyzed using Casa XPS  
141 software package. It bears emphasizing again that it is the surface (and not the total) oxygen, the only  
142 one able to interact with the water molecules during the first stages of the water sorption process.  
143 Hence, XPS is a more appropriate technique than elemental analysis to evaluate the oxygen located

144 on the surface of the carbonaceous materials (moreover taking into account that during the plasma  
145 treatment only the external surface of the samples is being modified [23, 24]). In the case of  
146 cement-bound materials, also the theoretical surface oxygen content was calculated. Finally, the  
147 porous character of the samples was verified by means of  $N_2$  adsorption at 77 K.

### 148 3. Results

149 First of all, characteristic water isotherms of the three groups of carbonaceous materials studied  
150 herein are shown in Figure 1a. As it can be observed, they present different shapes and water uptakes  
151 according to their textural properties and surface chemistry. As it has been indicated before, the water  
152 sorption process is initially driven by the hydrogen bonding between the water molecules and the  
153 surface functionalities and the subsequent cluster growth. Thus, in the range of the water isotherm  
154 fitted by the proposed equation (Figure 1b), only the surface chemistry of the material, and not its  
155 textural properties, is playing a role.



156

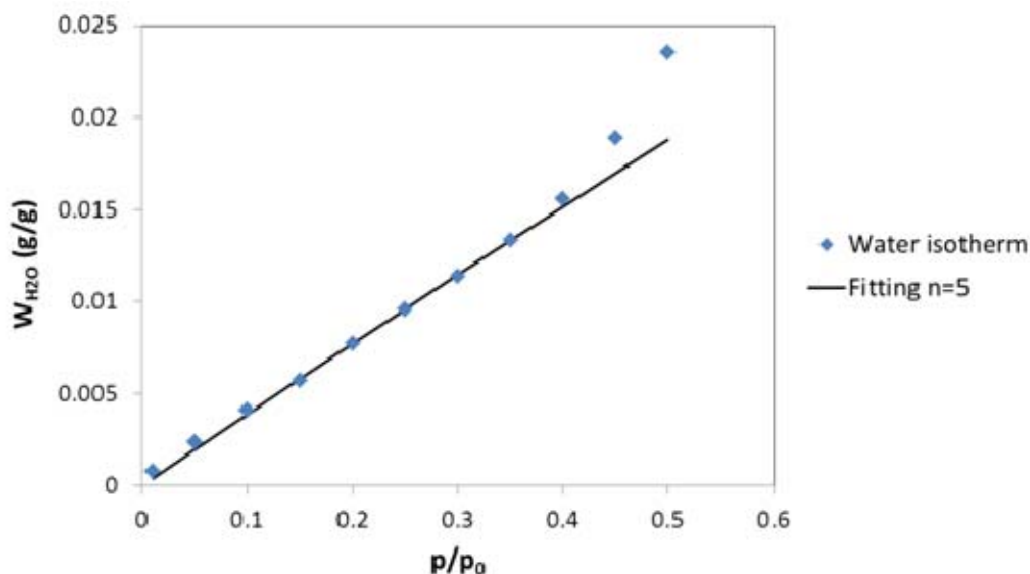
157 **Figure 1.** Complete (a) and low-pressure range (b) water isotherms of samples: 362, CR85 and  
158 CP 0.50.

159 This interval can be easily delimited since once the non-specific interactions prevail over the specific  
160 ones or, in other words, the pore filling begins, there is an upswing in the water isotherm (see Figure  
161 1b) that cannot be fitted by the proposed Langmuir-type equation [12]. In this way, the upper limit has

162 to be determined independently for every sample, and it does not necessarily coincide with the  
163 closure of the hysteresis loop, as we know water sorption sometimes exhibits low pressure hysteresis  
164 [26].

### 165 3.1. Carbon materials with high oxygen contents

166 Bearing in mind that in the earlier study [12] the validity of Eq. 1 was only verified for activated  
167 carbons up to 16 wt. % O, the first step in the current investigation was to check its suitability for  
168 other carbon materials within that surface oxygen content range. For this reason, sample CR70 was  
169 pyrolyzed at high temperature (700°C), aiming at considerably lowering its surface oxygen content.  
170 Hence, sample CR70 H700, with a surface oxygen content of 9.1 wt. % (XPS analysis), was obtained.  
171 Subsequently, its water sorption isotherm was measured and the fit of Eq.1 is shown in Figure 2.  
172 There it can be seen that at relative pressures lower than 0.4, the model assuming a cluster size of 5  
173 water molecules perfectly matches the experimental adsorption data and, as expected, the fitting is  
174 getting worse as the non-specific interactions (pore filling) take over from the specific interactions  
175 and the cluster formation. In fact, the estimated [O] value from the water isotherm is 8.9 wt. %, which  
176 is in perfect agreement with the surface oxygen content measured by XPS. This result further  
177 confirms the validity of the initially proposed model for carbonaceous materials (not only activated  
178 carbons) with low and moderate surface oxygen contents (< 16 wt. % O).



179



180 **Figure 2.** Fit of the water sorption isotherm of sample CR70 H700 with Eq. 1 assuming a cluster size  
181 of 5 water molecules.

182 Once this has been proven, we could move to the second (and main) objective of this research: to  
183 evaluate the model for the prediction of the low pressure range of the water sorption isotherms of  
184 highly hydrophilic carbon materials. To attain this goal, the water isotherms of the: i) parent  
185 carbonaceous resins (CR70 and CR85), ii) thermally modified CR70 at 200 and 450°C and iii) plasma  
186 treated samples, were measured. In this way, a series of carbons with surface oxygen contents ranging  
187 from 17 to 42 % in weight were analyzed. Then, the amount of surface oxygen calculated by the  
188 fitting with Eq. 1 was compared with the one resulting from direct XPS measurements (Table 2).  
189 There, it can be seen that for all the samples the oxygen contents estimated from the water sorption  
190 isotherm are lower than the XPS ones and the difference between both values increases with the  
191 hydrophilicity of the studied material. Therefore, the proposed model, assuming that a water cluster  
192 of 5 molecules ( $n=5$ ) is formed before the micropore filling, seems not to be valid for this kind of  
193 materials.

Sample	[Oxygen] (wt. %)		n parameter
	XPS	H <sub>2</sub> O isotherm	
<b>362</b>	16.9	16.2	4.6
<b>CR70 H450</b>	17.8	16.2	4.2
<b>362 PO2</b>	21.9	19.5	4.3
<b>CR70 H200</b>	24.3	20.2	4.0
<b>CR70 H450 PO2</b>	27.8	22.0	3.7
<b>362 PAr</b>	29.5	22.5	3.6
<b>CR70</b>	30.9	21.9	3.5
<b>CR85</b>	31.9	22.1	3.4
<b>CR70 PAr 1</b>	35.9	25.7	2.6
<b>CR70 PAr 2</b>	37.4	24.7	2.2
<b>CR70 H450 PAr</b>	39.6	20.6	1.9
<b>CR70 PO2</b>	41.9	19.5	1.1

194 **Table 2.** Comparison of the surface oxygen contents obtained by XPS and modelling of the water  
195 isotherms of the parent and modified carbon materials; as well as the n parameter for  
196 reverse fitting.

197 Considering this premise, the next step was to reverse the fitting procedure, taking into consideration  
198 the experimental oxygen content and calculating the size of the water cluster (n parameter). In this  
199 regard, n values between 4.6 and 1.1 were obtained (Table 2). Thus, again it can be noticed that there  
200 is a progressive fall in the n parameter value when analyzing samples with increasing surface oxygen  
201 content. It is also important to mention here that we have also reversed the fitting procedure for the  
202 activated carbon with the highest surface oxygen content that was included in the previous study  
203 (362) and we have found out that an n-value of 4.6 is more suitable. For the rest of the activated  
204 carbons, with lower amounts of oxygenated complexes on their surface, an n-factor of 5 is still  
205 applicable.

206 These results indicate that beyond a certain concentration of surface oxygen (ca. 16 wt. %) there is a  
207 gradual change in the water adsorption mechanism from clustering to layering. Considering the fact  
208 that oxygen-water interactions are always stronger than water-water interactions, water molecules  
209 will first bind to the oxygen groups located on the surface of the material, and only once there are no  
210 more available functionalities, the cluster formation and growth will begin. This phenomenon,  
211 enhanced by steric effects, will have an influence on the size of the water cluster formed before the  
212 micropore filling.

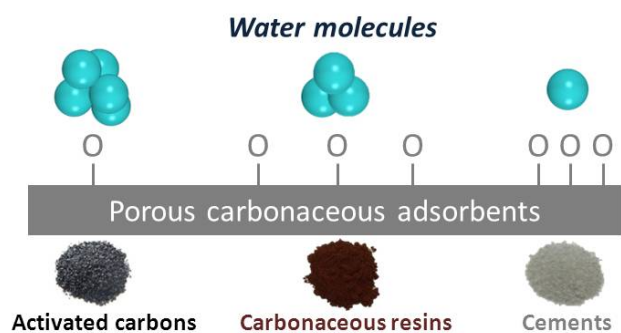
### 213 *3.2. Cement pastes*

214 As mentioned in the experimental section, two cement pastes with different water-to-cement ratios  
215 were prepared (CP 0.50 and CP 0.30). The high oxygen content (Table 3) of these materials also  
216 allowed us to go a little bit further in our study in terms of oxygen content. In addition, the absence of  
217 nitrogen within their composition (Table 3) helps us, once more, to separately study the effect of the  
218 surface oxygen complexes.

	XPS (wt. %)					H <sub>2</sub> O isotherm	
	C	S	Ca	Si	O	O (wt. %)	n value
<b>CP 0.30</b>	17.0	2.0	30.7	6.2	44.2	12.3	0.5
<b>CP 0.50</b>	20.0	1.6	28.3	6.8	43.4	14.0	0.6

219 **Table 3.** XPS analysis of the cement pastes included in this study (CP 0.50 and CP 0.30), and surface  
220 oxygen content and n parameter calculated from the fitting of their water sorption  
221 isotherms.

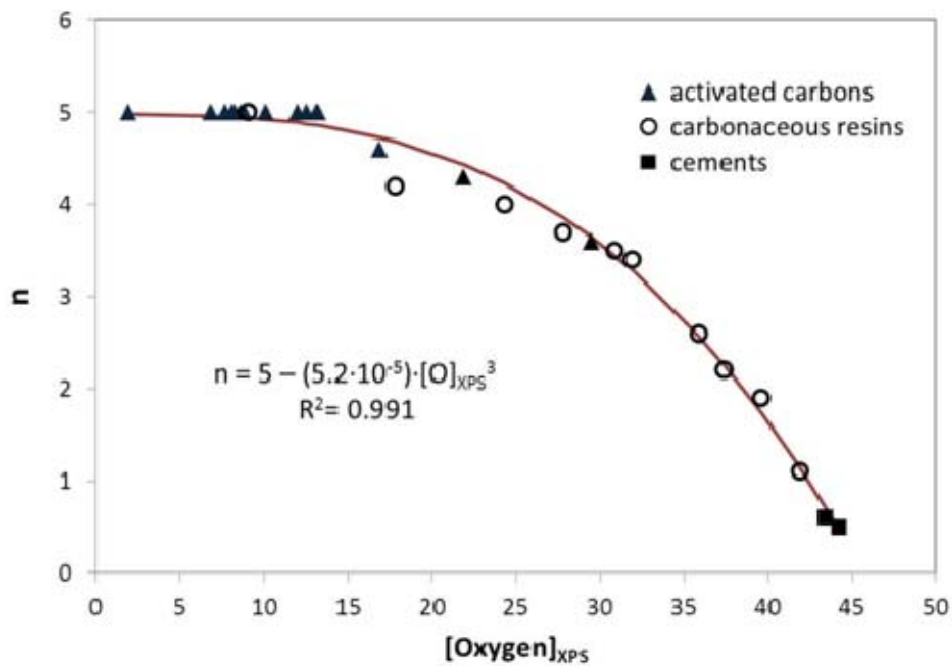
222 In Table 3 it is shown that the differences between the experimental (XPS) and the calculated values  
223 (Eq. 1 with  $n = 5$ ) for the surface oxygen contents are even more pronounced for these types of  
224 materials. Thus, when calculating the number of molecules in the water cluster by fixing the  $[O]_{XPS}$ ,  
225 the obtained values are lower than unity. However, and even though XPS has a penetration depth of  
226 only a few nanometers [27], it is highly probable that not all the oxygen quantified by this technique is  
227 available to participate in the adsorption mechanism. A plausible reason is that the complex structure  
228 of cements, and more precisely, the presence of bridging and non-bridging oxygen [28], hinders the  
229 selective quantification of surface oxygen groups. Furthermore, the theoretical oxygen content was  
230 calculated through the chemical composition of the CEM I 52.5 N cement [17,25] and slightly higher  
231 values than the experimental ones were obtained (46.6 and 52.3 % wt. O for samples CP 0.50 and CP  
232 0.30, respectively). This result points out to the possibility that the difference between the  
233 experimental and the theoretical oxygen contents corresponds to the oxygen located in the inner  
234 cement matrix. But, even if XPS somehow slightly overestimates the amount of surface oxygen  
235 complexes playing a role in the water sorption phenomenon, the calculated number of molecules in  
236 the water cluster (n) will be only marginally influenced and will certainly not go up much ( $n \leq 1$ ).  
237 According to this, it seems that there is an incomplete surface coverage and pore filling in these  
238 cementitious materials is not preceded by cluster formation of the water molecules. This is probably  
239 due to the much less hydrophobic nature of the pore walls compared to activated carbons. A  
240 schematic illustration of the herein obtained results is shown in Figure 3.



241

242 **Figure 3.** Schematic illustration of the influence of the surface oxygen content on the water cluster  
 243 size.

244 Finally, when representing the calculated n-values versus the oxygen content determined by XPS of  
 245 all the studied materials, and also including the activated carbons that were used in the previous work  
 246 [12], it is clear that all the samples (including the cements) follow the same descending trend  
 247 (Figure 4). Moreover, it is possible to obtain a simple numerical fitting, based on a third degree  
 248 polynomial function (inset in Figure 4). In this regard, the obtained numerical parameters seem to be  
 249 logical since the n-value tends to be 5 as the surface oxygen content is decreased, which is the number  
 250 of water molecules forming the cluster before the micropore filling for those activated carbons with  
 251 an oxygen content lower than 16 wt. %. And also the order of the function (power of 3) is in  
 252 agreement with the fact that an increasing three-dimensional hindering is taking place as the surface  
 253 oxygen content is increased.



254

255 **Figure 4.** Modeling of the influence of the surface oxygen content on the cluster size.

256 Summarizing, it was found that when the surface oxygen content of porous carbonaceous materials is  
 257 higher than 16 wt. %, the calculated n-values begin to progressively decrease, being  $\leq 1$  in the case of  
 258 the samples with the highest oxygen contents (cements). These results indicate that in those materials  
 259 with very high surface oxygen contents, steric effects become important, thus having also an  
 260 influence on the size of the water cluster formed before the micropore filling. Consequently, for  
 261 highly hydrophilic carbon materials it is necessary to adapt the value of the cluster size (n) in order to  
 262 predict the first part of the water sorption isotherms using independent surface oxygen measurements  
 263 (e.g. XPS).

264 **4. Conclusions**

265 This work provides further insights into the influence of the surface oxygen content of porous  
 266 carbonaceous materials on the mechanisms prevailing at the beginning of the water sorption process.  
 267 It has been shown that beyond a certain concentration of surface oxygen content ( $\sim 16$  wt. %), there is  
 268 a change in the sorption mechanism (from clustering to layering), enhanced by steric effects. Hence,  
 269 the size of the water cluster, formed before the micropore filling starts, steadily decreases from the

270 initial value of 5. Furthermore, the presence of very high amounts of oxygenated groups on the  
271 surface of the sample (i.e. cements) inhibits the occurrence of water-water interactions and therefore  
272 the formation of water clusters.

273 Therefore, Equation 1 is valid if  $n$  is adapted as a function of the oxygen content according to the  
274 function:  $n = 5 - (5.2 \cdot 10^{-5}) \cdot [\text{O}]_{\text{XPS}}^3$ .

275

## 276 **Acknowledgements**

277 As a Research Assistant of the Research Foundation-Flanders (FWO-Vlaanderen), D. Snoeck wants  
278 to thank the foundation for the financial support (1.1.D74.15N). The authors also want to thank the  
279 Research Foundation-Flanders for funding the project entitled ‘Effect of Tunable Hydrogels on  
280 Concrete Microstructure, Moisture Properties, Sealing and Self-Healing of Cracks’ (3G019012).

281

## 282 **REFERENCES**

- 283 [1] Furmaniak S, Gauden PA, Terzyk AP, Rychlicki G. Water adsorption on carbons. Critical review  
284 of the most popular analytical approaches. *Adv. Coll. Interf. Sci.* 2008; 137: 82–143.
- 285 [2] Czakkel O, Dobos G, Lodewyckx P, Rochas C, Geissler E. Water vapour adsorption in highly  
286 porous carbons as seen by small and wide angle X-ray scattering. *Carbon* 2010; 48: 1038–48.
- 287 [3] Nguyen TX, Bhatia SK. How water adsorbs in hydrophobic nanospaces. *J. Phys. Chem. C* 2011;  
288 115: 16606–12.
- 289 [4] Tóth A, László K. Water adsorption by carbons: hydrophobicity and hydrophilicity. In: Tascón  
290 JMD, editor. *Novel Carbon Adsorbents*, Amsterdam; Elsevier; 2012, p. 147–71.
- 291 [5] Horikawa T, Muguruma T, Do DD, Sotowa KI, Alcántara-Ávila JR. Scanning curves of water  
292 adsorption on graphitized thermal carbon black and ordered mesoporous carbon. *Carbon* 2015;  
293 95: 137–43.

- 294 [6] Thommes M, Morell J, Cychosz KA, Fröba M. Combining nitrogen, argon and water adsorption  
295 for advanced characterization of ordered mesoporous carbons (CMKs) and periodic mesoporous  
296 organosilicas (PMOs). *Langmuir* 2013; 29: 14893–902.
- 297 [7] Horikawa T, Zeng Y, Do DD, Sotowa KI, Alcántara-Ávila JR. On the isosteric heat of adsorption  
298 of non-polar and polar fluids on highly graphitized carbon black. *J. Colloid Interface Sci.* 2015;  
299 439: 1–6.
- 300 [8] Do DD, Do HD. A model for water adsorption in activated carbon. *Carbon* 2000; 38: 767–73.
- 301 [9] Cossarutto L, Zimny T, Kaczmarczyk J, Siemienieska T, Bimer J, Weber JV. Transport and  
302 sorption of water vapour in activated carbons. *Carbon* 2001; 39: 2339–346.
- 303 [10] Ohba T, Kanoh H, Kaneko K. Structures and stability of water nanoclusters in hydrophobic  
304 nanospaces. *Nano Lett.* 2005; 5: 227–30.
- 305 [11] Oubal M, Picaud S, Rayez MT, Rayez JC. A theoretical characterization of the interaction of  
306 water with oxidized carbonaceous clusters. *Carbon* 2010; 48: 1570–9.
- 307 [12] Lodewyckx P, Raymundo-Piñero E, Vaclavikova M, Berezovska I, Thommes M, Béguin F,  
308 Dobos G. Suggested improvements in the parameters used for describing the low relative  
309 pressure region of the water vapour isotherms of activated carbons. *Carbon* 2013; 60: 556–8.
- 310 [13] Thommes M, Morlay C, Ahmad R, Joly JP. Assessing surface chemistry and pore structure of  
311 active carbons by a combination of physisorption (H<sub>2</sub>O, Ar, N<sub>2</sub>, CO<sub>2</sub>), XPS and TPD-MS.  
312 *Adsorption* 2011; 17: 653–61.
- 313 [14] Nguyen VT, Horikawa T, Do DD, Nicholson D. Water as a potential probe for functional groups  
314 on carbon surfaces. *Carbon* 2014; 67: 72–78.
- 315 [15] Zeng Y, Prasetyo L, Nguyen VT, Horikawa T, Do DD, Nicholson D. Characterization of oxygen  
316 functional groups on carbon surfaces with water and methanol adsorption. *Carbon* 2015; 81:  
317 447–57.
- 318 [16] Jennings HM, Bullard JW. From electrons to infrastructure: Engineering concrete from the  
319 bottom up. *Cement Concrete Res.* 2011; 41: 727–35.

- 320 [17] Snoeck D, Velasco LF, Mignon A, Van Vlierberghe S, Dubruel P, Lodewyckx P, De Belie N.  
321 The influence of different drying techniques on the water sorption properties of cement-based  
322 materials. *Cem. Concr. Res.* 2014; 64: 54–62.
- 323 [18] Thomas JJ, Allen AJ, Jennings HM. Structural changes to the calcium-silicate-hydrate gel phase  
324 of hydrated cement with age, drying, and resaturation. *J. Am. Ceram. Soc.* 2008; 91(10): 3362–9.
- 325 [19] Pekala RW. Organic aerogels from the polycondensation of resorcinol with formaldehyde. *J. Mat.*  
326 *Sci.* 1989; 24(9): 3221–7.
- 327 [20] Haro M, Rasines G, Macías C, Ania CO. Stability of a carbon gel electrode when used for the  
328 electro-assisted removal of ions from brackish water. *Carbon* 2011; 49: 3723–30.
- 329 [21] Seredych M, Ania C, Badosz TJ. Moisture insensitive adsorption of ammonia on  
330 resorcinol-formaldehyde resins. *J. Hazard. Mater.* 2016; 305: 96–104.
- 331 [22] Isaacs Páez E, Haro M, Juárez-Pérez EJ, Carmona RJ, Parra JB, Leyva Ramos R, Ania CO. Fast  
332 synthesis of micro/mesoporous xerogels: Textural and energetic assessment. *Microp. Mesop.*  
333 *Mat.* 2015; 209: 2–9.
- 334 [23] García AB, Martínez-Alonso A, León y León CA, Tascón JMD. Modification of the surface  
335 properties of an activated carbon by oxygen plasma treatment. *Fuel* 1998; 77(6): 613–24.
- 336 [24] López-Garzón FJ, Domingo-García M, Pérez-Mendoza M, Alvarez PM, Gómez-Serrano V.  
337 Textural and chemical surface modifications produced by some oxidation treatments of a glassy  
338 carbon. *Langmuir* 2003; 19(7): 2838–44.
- 339 [25] Snoeck D, Velasco LF, Mignon A, Van Vlierberghe S, Dubruel P, Lodewyckx P, De Belie N.  
340 The effects of superabsorbent polymers on the microstructure of cementitious materials studied  
341 by means of sorption experiments. *Cem. Concr. Res.* 2015; 77: 26–35.
- 342 [26] Velasco LF, Guillet-Nicolas R, Dobos G, Thommes M, Lodewyckx P. Towards a better  
343 understanding of water adsorption hysteresis in activated carbons by scanning isotherms. *Carbon*  
344 96 (2016) 753-8.



345 [27]Horgnies M., Chollet M. Composition of concrete surfaces after demoulding and coating:  
346 comparative study by XPS, FTIR and Raman spectroscopies. Key Eng. Mater. 2011; 466:  
347 215–23.

348 [28]Kurdowski W. Cement and Concrete Chemistry. Springer Netherlands, 2014.  
349 ISBN: 978-94-007-7944-0.

350

351 **Figures captions.**

352 **Figure 1.** Complete (a) and low-pressure range (b) water isotherms of samples: 362, CR70 and  
353 CP 0.50.

354 **Figure 2.** Fit of the water sorption isotherm of sample CR70 H700 with Eq. 1 assuming a cluster size  
355 of 5 water molecules.

356 **Figure 3.** Schematic illustration of the influence of the surface oxygen content on the water cluster  
357 size.

358 **Figure 4.** Modeling of the influence of the surface oxygen content on the cluster size.

359

360

361 **Tables captions.**

362 **Table 1.** Surface chemistry characterization of the carbonaceous resins (CR70 and CR85).

363

364 **Table 2.** Comparison of the surface oxygen contents obtained by XPS and modelling of the water  
365 isotherms of the parent and modified carbon materials; as well as the n parameter for reverse fitting.

366

367 **Table 3.** XPS analysis of the cement pastes included in this study (CP 0.50 and CP 0.30), and surface  
368 oxygen content and n parameter calculated from the fitting of their water sorption isotherms.

369

370